JOURNAL OF CATALYSIS 109, 387–395 (1988)

Nickel and Vanadium on Equilibrium Cracking Catalysts by Imaging Secondary Ion Mass Spectrometry

E. L. KUGLER AND D. P. LETA

Exxon Research & Engineering Company, Route 22 East, Clinton Township, Annandale, New Jersey 08801

Received August 12, 1987; revised September 23, 1987

The distribution of nickel and vanadium has been determined on refinery samples of several types of fluidized catalytic cracking catalyst. Data from imaging secondary ion mass spectrometry show that metals in catalytic cracking feedstocks initially deposit near the external surface of catalyst particles. Nickel remains in the area where it was deposited, while vanadium shows both intraparticle and interparticle mobility. Vanadium accumulates throughout catalyst particles, but shows a preference for both rare earth exchanged Y-zeolite and alumina phases in composite catalyst. By contrast, nickel shows no preference for catalyst phases and accumulates monotonically with time. The lack of mobility in deposited nickel makes it a good measure to determine the age of individual particles. © 1988 Academic Press, Inc.

INTRODUCTION

Metals in hydrocarbon feedstocks can deposit on processing catalysts and change catalyst performance with time. With fluidized catalytic cracking (FCC), nickel and vanadium in feeds accumulate quantitatively on catalyst particles and severely affect unit operations. Both metals increase hydrogen and coke and decrease gasoline yields. Metal contamination on catalyst particles is usually limited to moderate levels through choice of feedstocks for the FCC unit, or by charging enough fresh catalyst daily to maintain an optimum equilibrium concentration of deposited metals. However, at some locations, refinery economics or lack of other processing options requires that heavy feeds high in metals be converted in a catalytic cracking unit. The necessity or the desirability of processing high-metal feeds in an FCC unit has generated much research on how metals affect catalyst particles and how metal effects can be controlled.

Early examinations of metal effects focused on increased hydrogen and coke produced by nickel and vanadium (*1–10*). More recently, Ritter and co-workers (*11*) observed that vanadium also affected catalyst activity by destroying zeolite structures. Confirmation of the role of vanadium in attacking zeolites was made by X-ray powder diffraction measurements. Elemental imaging techniques showed the association of vanadium with zeolite. Jaras (*12*) used secondary ion mass spectrometry (SIMS) to show the distribution of vanadium on laboratory samples before and after severe steaming. Vanadium, evenly distributed throughout the catalyst particle on preparation, migrated and concentrated at the location of the rare earth exchanged zeolite after steaming. Although the elemental images produced by vanadium and lanthanum ions were very similar after hydrothermal treating, the nickel distribution did not change. It remained evenly distributed throughout the sample.

Similar mapping studies have been made using electron microprobe techniques. Masuda *et al.* (*13, 14*) used electron microprobe analysis on cross-sectioned catalyst particles to show that vanadium and lanthanum were again concentrated in the same regions in steam deactivated catalysts with rare earth Y-zeolites. Nickel was evenly distributed throughout the particle in these laboratory prepared samples. Similar work described by Maselli and Peters

0021-9517/88 $3.00

(*15*) also showed a correlation between vanadium and rare earths when the catalyst matrix contained silica and clay. However, this correlation disappeared when the catalyst matrix was a high-surface-area silica–alumina. With the silica–alumina matrix, vanadium remained well distributed throughout the catalyst. Research by Pompe *et al.* (*16*) suggests that rare earth exchanged zeolites form rare earth vanadates, accounting for the observed proximetry between lanthanum and vanadium in catalysts containing rare earths. The role of the silica–alumina matrix in keeping vanadium well distributed was not fully explained in the paper by Maselli.

All of the reports on vanadium attacking zeolite structures have been based on laboratory prepared samples. The protocol developed by Mitchell (*8*) to stimulate equilibrium catalyst performance provides good correlations as determined by microactivity test results (*9, 10*). To test the validity of elemental imaging data on laboratory prepared catalysts, we have chosen to examine equilibrium catalysts from commercial operation. Since commercial practice requires that fresh catalyst be added daily to make up inventory that was lost through attrition or discarded to control metal levels, equilibrium catalyst will contain particles with a range of ages and metal concentrations. Most units add 1 to 3% fresh catalyst daily to the unit inventory. This would suggest that the average particle residence time were 33 to 100 days. However, within any given sample, we might expect to find some particles that have been in the unit less than 1 day and other particles that have been present for 6 months. The wide range of particle ages provides the opportunity to observe how metal distributions might change as a particle ages. The actual age of any particle cannot be determined, but particles with low metals, particularly nickel which is immobile, are probably new while others with high nickel must be older.

Imaging secondary ion mass spectrometry was used to study elemental distributions on particle cross sections because of its high sensitivity to most metals found in cracking catalysts. This sensitivity varied from one element to another, but in general, is 100- to 1000-fold greater than that possible with electron microprobe measurements. Spatial resolution of less than 0.5 μm is attainable, several times better than is possible with electron microprobe. One shortcoming of our imaging SIMS measurements is that they are not quantitative, due to matrix effects in the ion formation process, which our image handling capabilities cannot yet correct.

METHODS

The samples analyzed by SIMS in this study were first embedded in copper-doped thermosetting epoxy to provide increased electrical conductivity. The epoxy was dry mixed with the sample prior to thermosetting and did not penetrate the catalyst particles. The epoxy mounted samples were then dry polished with silicon carbide to 600 grit to approximate cross sections. Standard wet polishing techniques were not used to avoid altering the distribution of metals with common solvents. The SIMS analyses were performed using a CAMECA IMS-3F ion microprobe/microscope, equipped with a single ion selectivity, high-resolution imaging system described elsewhere (*17*). Oxygen as O_2^+ was used as the primary ion bombardment species, at an impact energy of 10.5 keV.

In order to eliminate the effects of polishing damage and contamination on the surfaces, samples were presputtered to a depth of several micrometers before elemental images were collected. For most images, integration times of 8 to 30 s were sufficient to provide reasonable signal-to-noise on the final images. All of the elemental images are normalized to a standard brightness for viewability. As such, brightness within one image may be used to gauge an element's relative concentration from area to area, but no conclusions should be drawn be-

tween different images without using the mass spectral count rates.

RESULTS AND DISCUSSION

Fluid catalytic cracking catalyst particles can be examined element by element using imaging SIMS techniques. The only prior study of cracking catalyst with this technique (*12*) used catalyst samples containing zeolite and kaolin spray dried with a silica sol binder. Laboratory addition of nickel and vanadium, followed by high-temperature steaming, produced a catalyst where the nickel was evenly distributed throughout the sample, but the vanadium was associated with the rare earth exchanged Y-zeolite. We have examined a similarly composed catalyst from commercial operation with metals deposited by processing heavy oils. The average metal concentration in this sample is 1500 ppm nickel and 3340 ppm vanadium. The zeolite concentration in fresh catalyst is about 20%. Ion images from this sample are shown in Fig. 1.

Silicon or aluminum ion images are most useful for locating catalyst particles with the SIMS technique. Both the zeolite and kaolin components are aluminosilicates, so either ion will show the full size of the particle. Figure 1a is the silicon ion image produced at a magnification of 400×. The field of view is 150 μm from top to bottom so that the particle size of the catalyst shown is about 60 μm. The brighter areas indicate

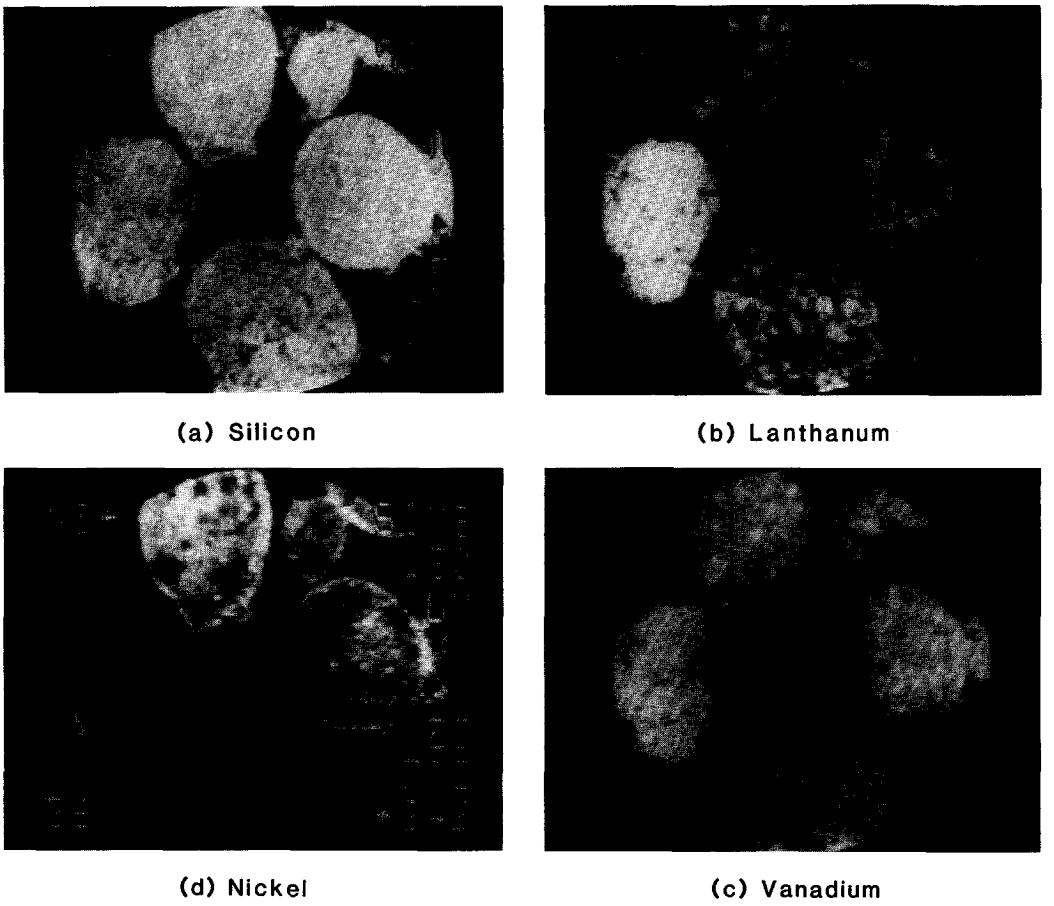

FIG. 1. Cross sections of catalyst containing zeolite and kaolin particles. Ion images show (a) silicon, (b) lanthanum, (c) vanadium, and (d) nickel.

higher concentrations of the ion imaged. The silicon image has variations in brightness on particles at the bottom and at the left side of the photograph that give the appearance of many small particles being cemented together. This is in fact how these same particles appear in scanning electron microscope pictures.

The locations of the zeolite are revealed by images produced by rare earth elements that have been exchanged into the zeolite. The lanthanum image, Fig. 1b, shows that the zeolite concentrations in these catalyst particles vary widely. The particle on the left seems to be nearly all zeolite, and the one on the bottom shows high zeolite concentration but as discrete aggregates of smaller zeolite crystals, while the other particles have lower concentrations of zeolite as marked by the lanthanum image.

The vanadium ion image discloses the correspondence between the lanthanum and the vanadium. The particle at the bottom of the photograph indicates almost a perfect overlay between the vanadium and the lanthanum images. The same is true for the particle at the left that is either all zeolite or contains well-dispersed zeolite crystallites rather than zeolite aggregates. The particles at the top of the photograph show that vanadium can be all over the particle even though only a small portion is zeolite. However, the fact that vanadium is concentrated in zeolite particles is revealed by brighter spots in the vanadium image. These photographs clearly show a preference of vanadium for zeolite in a catalyst composed of only zeolite, kaolin, and silica binder. However, they also show that vanadium may equilibrate at locations other than on the zeolite crystals.

The nickel ion image in Fig. 1d shows several particles with high nickel concentrations while others have very low nickel signals. The nickel concentration probably reflects the time a particle has been in a unit (*18*). The particle at the bottom of the photograph and the one on the left show very little nickel so that we must conclude that these catalyst particles have been in the unit only a short time even though they have high vanadium concentrations. The particles at the top have high nickel concentrations, enhanced at the edges. These particles must be much older than the ones at the bottom. Of particular interest in these nickel images are the dark areas in the older particles. These dark areas are at the location of the zeolite aggregates suggesting that the nickel cannot gain access to the zeolite crystals, in contradistinction to the behavior of the vanadium that can migrate into the zeolite. This further suggests that the nickel resides, immobile, at the location where the nickel porphyrins decomposed.

The high vanadium concentrations on catalyst particles that have a very low nickel age suggest that vanadium not only has mobility across catalyst particles but that it also has interparticle mobility. Wormsbecher *et al.* have suggested that vanadium may be transported through the vapor phase (*19*). Interparticle transport would also seem reasonable through particle contacting in the fluidized bed of the FCC regenerator.

Cracking catalyst containing only zeolite, clay, and binder is commonly used for gas oil conversion, but would be atypical of catalysts used for cracking heavier feeds. Resid conversion catalysts usually have some high-surface-area, large-pore-size component for large molecule cracking. The catalyst examined in Fig. 2 uses mixtures of particles to obtain surface area accessible to large molecules. One kind of particle in the mixture is clay and a binder that has been spray dried and then thermally and chemically treated to enhance activity. The other type of particle contains zeolite synthesized on the same clay base.

Images from many catalyst particles are shown in Fig. 2. The magnification is about 160×, with the field of view from top to bottom being approximately 400 μm. The individual particles vary in size from 20 to 120 μm. The silicon image, shown in Fig. 2a, is the most useful for finding particles

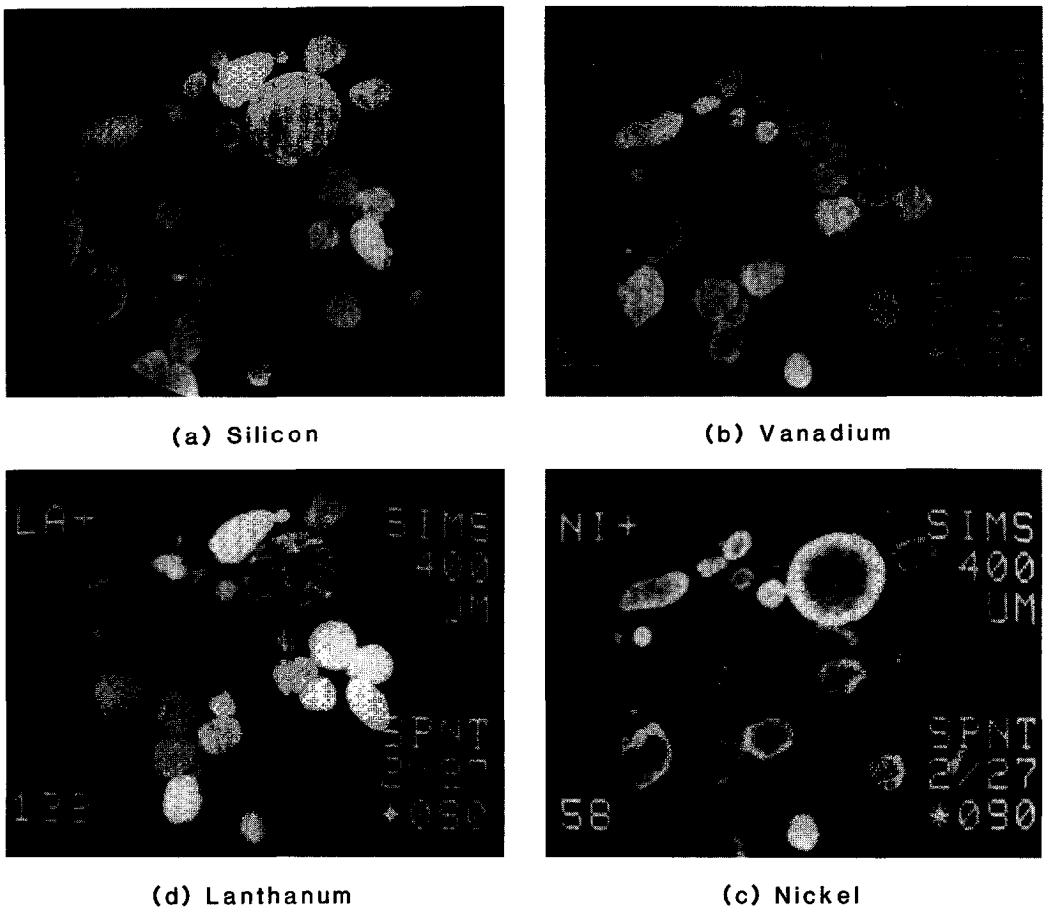

FIG. 2. Cross sections of equilibrium catalyst containing a mixture of particle types. Ion images show (a) silicon, (b) vanadium, (c) nickel, and (d) lanthanum.

and shows their individual sizes and shapes.

The vanadium ion image in Fig. 2b reveals substantial variations from particle to particle. The average vanadium concentration on this sample is 2060 ppm. However, the ion image shows that some particles have an even intensity whereas others have high concentrations near the outside rim with very little vanadium on the interior of the particle. The even distributions of vanadium across a cracking catalyst particle are consistent with intraparticle vanadium mobility. The particles with the rim distributions appear to have spent less time in the unit so that vanadium has not penetrated the catalyst, or to have immobilized vanadium by some means near the external surface.

The distribution of nickel on this same catalyst sample is shown in Fig. 2c. The average nickel concentration in the sample is 790 ppm. The nickel ion image shows that nickel is concentrated near the particle edge in nearly all of the particles examined. The particles with higher nickel concentrations have probably been in the unit longer than those with only low concentrations on the particle rim.

The lanthanum ion image in Fig. 2d provides additional information about the mixture of particles comprising equilibrium catalyst. The lanthanum ions show that most of the particles have an even distribution of

rare earth exchanged zeolite whereas one shows discrete zones within the particle. The large particle with discrete zones can be identified as a remnant of catalyst prepared by a different manufacturing technique that had previously been in the unit and is at least 15 months old. The particles with even brightness are catalyst that is currently being added on a daily basis. The even intensity means that the zeolite crystallites are well distributed as determined at an instrument resolution of 0.5 μm. Some of the particles contain no rare earths at all. These treated clay particles in the catalyst mixture can be found by comparing the lanthanum ion image with the silicon image that reveals all the particles of the mixture.

As stated above, the lanthanum ion distribution revealed one particle that had been in the unit for 15 months or more. This same particle in Fig. 2c has a very high nickel concentration, but still has more nickel near the exterior rim of the catalyst than in its interior. The concentration of nickel near the outside surfaces of catalyst particles suggests that the nickel containing molecules in the feedstock decomposed soon after contacting the particle and that deposited nickel has, at best, low mobility across the catalyst particle. The vanadium image of the older particle has similar brightness with many other particles that are much younger. This is another example that vanadium concentration on an individual particle is not a good measure of catalyst age.

Many catalysts designed for heavy feed processing contain alumina particles in addition to zeolite and clay. The alumina appears to provide surface area that is available to larger molecules, molecules that are too large to have direct access to the pore structure of the zeolite. An example of a catalyst containing alumina is provided in Fig. 3, where a magnification of 400× provides a top to bottom field of view of approximately 150 μm.

The silicon ion image of Fig. 3a shows many dark areas within the catalyst particles that mark the position of particulate alumina. These same areas are bright in the aluminum ion image, but that picture has not been included since there is poor contrast between the particulate alumina and the rest of the catalyst particle.

The vanadium ion image, Fig. 3b, shows that vanadium has spread throughout the catalyst particle, but has accumulated on the particulate alumina. Comparing the vanadium and silicon ion images reveals that the dark spots on the silicon image correspond directly to the brighter spots of the vanadium image. This could indicate that heavy molecules containing vanadium crack on the particulate alumina, or it may indicate that vanadium prefers to reside on the alumina, perhaps by reacting to form aluminum vanadate in the FCC regenerator.

The lanthanum ion image in Fig. 3c shows no direct correlation between the vanadium and the rare earth in this sample. The correspondence between the vanadium and the alumina positions, and the lack of correspondence between the vanadium and the rare earth, indicate a preference of the vanadium for the alumina over the zeolite particles. However, older particles, as determined by their nickel concentrations, often show vanadium on both the zeolite and the alumina phases.

The nickel ion image in Fig. 3d shows that nickel has accumulated primarily at the catalyst edge. The low nickel concentration suggests that all of these particles have been in the unit only a short time.

A last example of metal distributions on equilibrium cracking catalyst is provided in Fig. 4. As in the previous example, the catalyst contains alumina as well as the usual zeolite, kaolin, and silica binder. In this case, the silicon ion image shows not only dark areas indicating the alumina particulates but also two bright rings showing where two smaller particles were encapsulated during catalyst manufacture. The aluminum ion image, Fig. 4b, and the vanadium ion image, Fig. 4c, are almost

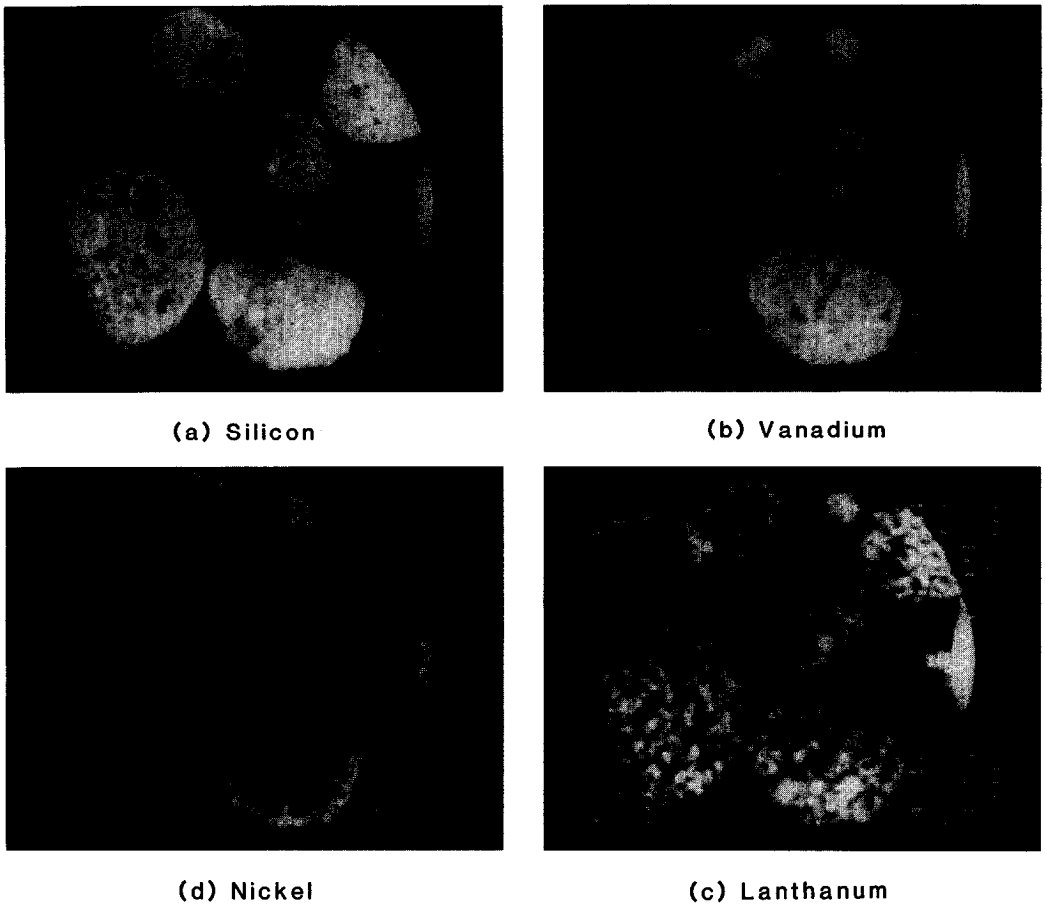

FIG. 3. Cross sections of equilibrium catalyst containing alumina, zeolite, and kaolin particulates. Ion images show (a) silicon, (b) vanadium, (c) lanthanum, and (d) nickel.

identical showing the accumulation of vanadium on the particulate alumina. However, substantial contrast may be seen on the nickel ion image. In this case, nickel has penetrated the particle and appears to have higher concentrations on the alumina particles. However, very little nickel has penetrated the two encapsulated smaller particles. This lack of penetration may indicate that nickel porphyrins, or other nickel compounds in feeds, decompose primarily at a diffusion barrier. The first barrier encountered on cracking catalysts is the external particle skin. Most catalyst samples examined show nickel accumulated at the external surface. Older catalyst particles show that nickel penetrates the external surface. It is not clear whether deposited nickel has low mobility or whether changes in the catalyst with time allow greater penetration of nickel containing molecules into older particles. This last example, and certainly a minority example among the samples examined, indicates that where nickel loadings are high, nickel may accumulate on particulate alumina and on the binder phases within the catalyst particle.

CONCLUSIONS

Equilibrium catalysts accumulate feed metals quantitatively but the distribution of the metals on equilibrium catalyst is very dependent on catalyst type. Early reports (*12–15*) based on laboratory prepared sam-

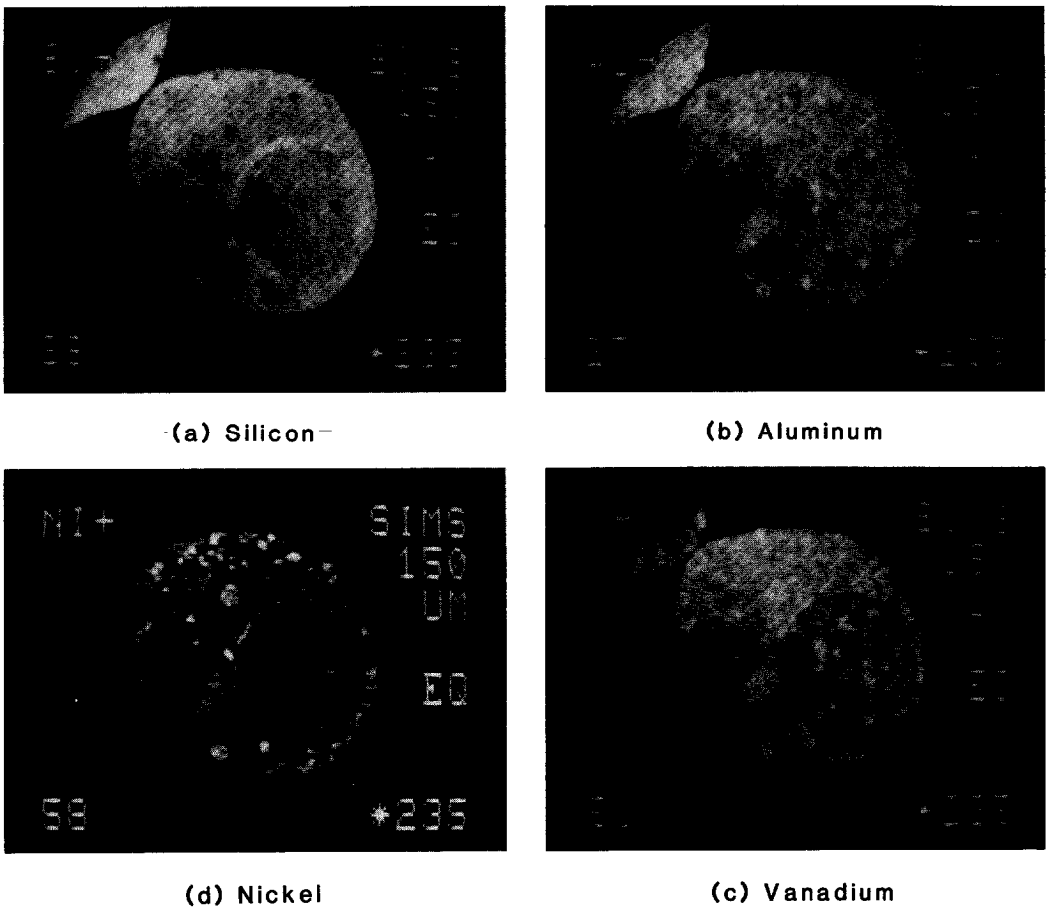

FIG. 4. Cross sections of equilibrium catalyst containing alumina, zeolite, and kaolin particles. Ion images show (a) silicon, (b) aluminum, (c) vanadium, and (d) nickel.

ples showed that vanadium migrated to rare earth exchanged zeolite crystals and that nickel remained where it was deposited from solution. Our observations with equilibrium catalysts are totally consistent for catalysts that contain only zeolite, kaolin, and silica binder. The vanadium migrates to the zeolite and the nickel seems to remain where it was deposited.

However, extensive examinations of equilibrium catalysts reveal much more detail about how metals interact with catalyst. Our data show that metals in feeds initially accumulate on surfaces accessible to large porphyrin-like molecules. This is primarily the external surface of the catalyst. Samples containing low concentrations of both nickel and vanadium show rim distributions at the external surface.

However, after initial deposition on the catalyst surface, nickel and vanadium differ substantially. Deposited nickel either is immobile or has only very low mobility, while deposited vanadium has high mobility. The practice of estimating a particle age from its nickel concentration appears to be quite valid, since even very old particles have edge-enhanced nickel distributions showing that it cannot move very rapidly. Vanadium mobility is quite high by comparison. Very few particles are observed with vanadium only on the particle edge. Vanadium has usually spread throughout a particle, even on those with very low nickel concentra-

tions. Particles with high vanadium concentrations but abnormally low nickel concentrations support hypotheses of interparticle vanadium transport. However, these examinations of equilibrium samples cannot provide data on whether particle-to-particle vanadium transport occurs through the vapor phase, or whether it occurs only through particle contacting.

Catalysts used for heavy feed conversion often contain particulate alumina. Vanadium accumulates preferentially on alumina although it is not isolated on the alumina phase. Vanadium may react with aluminum oxide to form aluminum vanadates. However, that phase is not expected to permanently trap vanadium, since aluminum vanadate is reported to melt incongruently starting at 700°C (*20*). The catalyst samples shown in Figs. 1–3 came from units with regenerator temperatures above the initial melting temperature reported for aluminum vanadate.

This study has demonstrated with equilibrium catalyst that many observations made with laboratory prepared samples are valid. It has shown that prior contentions about vanadium and nickel mobilities are certainly correct, but it has also shown that evenly distributed nickel and vanadium as obtained in the laboratory are far from reality. The standard hydrothermal aging techniques used to deactivate cracking catalysts redistribute vanadium so that lab and refinery samples should be nearly equivalent. Nickel added to catalyst in the laboratory does not resemble nickel added to catalyst under processing conditions. However, standard aging techniques still bring nickel activity in line with that of equilibrium catalyst (*8*), even though the actual nickel distributions between the two samples may be quite different.

ACKNOWLEDGMENTS

The authors thank Marena Brons for mounting and polishing samples for SIMS studies and acknowledge the efforts of many others who helped us obtain samples of equilibrium refinery catalyst.

REFERENCES

1. Mills, G. A., *Ing. Eng. Chem.* **42,** 182 (1950).
2. Duffy, B. J., and Hart, W. M., *Chem. Eng. Prog.* **48,** 344 (1952).
3. McEvoy, J. E., Milliken, T. H., Mills, G. A., *Ind. Eng. Chem.* **49,** 865 (1957).
4. Meisenheimer, R. G., *J. Catal.* **1,** 356 (1962).
5. Rothrock, J. J., Birkhimer, E. R., and Leum, L. N., *Ind. Eng. Chem.* **49,** 272 (1957).
6. Conner, J. E., Jr., Rothrock, J. J., Birkhimer, E. R., and Leum, L. N., *Ind. Eng. Chem.* **49,** 276 (1957).
7. Cimbalo, R. N., Foster, R. L., and Wachtel, S. J., *Oil Gas J.,* May 15, 112 (1972).
8. Mitchell, B. R., *Ind. Eng. Chem. Prod. Res. Dev.* **19,** 209 (1980).
9. Henderson, D. S., and Ciapetta, F. G., *Oil Gas J.,* October 16, 88 (1967).
10. ASTM Method D 3907-80 (1980).
11. Ritter, R. E., Rheaume, L., Welsh, W. A., and Magee, J. S., *Oil Gas J.,* July 6, 103 (1981).
12. Jaras, S., *Appl. Catal.* **2,** 207 (1982).
13. Masuda, T., Ogata, M., Ida, T., Takakura, K., and Nishimura, Y., *J. Japan. Pet. Inst.* **26,** 344 (1983).
14. Nishimura, Y., Masuda, T., Sato, G., and Egashira, S., *Prepr. Div. Pet. Chem. Amer. Chem. Soc.* **28,** 707 (1983).
15. Maselli, J. A., and Peters, A. W., *Catal. Rev. Sci. Eng.* **26,** 525 (1984).
16. Pompe, R., Jaras, S., and Vannerberg, N. G., *Appl. Catal.* **13,** 171 (1984).
17. Leta, D. P., "Springer Series in Chemical Physics 44" (A. Benninghoven, R. J. Colton, D. S. Simons, and H. W. Werner, Eds.), p. 232. Springer-Verlag, Berlin, 1986.
18. Palmer, J. L., and Cornelius, E. G., "Ninth North American Meeting of the Catalysis Society, Houston, TX," Paper A-36, 1985.
19. Wormsbecher, R. F., Peters, A. W., and Maselli, J. M., *J. Catal.* **100,** 130 (1986).
20. Reid, A. F., and Sabine, T. M., *J. Solid State Chem.* **2,** 203 (1970).